Atmospheric Pollution Research

Secondary organic aerosol over an urban environment in a semi–arid region of western India

Athiyarath K. Sudheer, Ramabadran Rengarajan, Varun Sheel

Physical Research Laboratory, Ahmedabad, 380 009, India

ABSTRACT

Carbonaceous species in PM_{10} and $PM_{2.5}$ samples, collected from an urban location at Ahmedabad in India during summer, were analyzed to study variability in water–soluble organic carbon (WSOC) and secondary organic carbon (SOC) along with atmospheric water vapor content. A significant correlation between WSOC and SOC was found indicating major contribution of soluble organic compounds by secondary organic aerosol formation. A strong inverse dependence of WSOC and SOC on atmospheric water vapor content is observed in both PM_{10} and $PM_{2.5}$ (at <45% relative humidity, RH) during daytime; whereas data collected during monsoon season at higher RH conditions do not exhibit such relation. Aerosol liquid water content (LWC) calculated from thermodynamic equilibrium model suggests that the decrease in secondary organic aerosol (SOA) with increase in RH occurs when LWC is absent or insignificant amount. The inverse correlation in summertime indicates possible decrease in the extent of heterogeneous photochemical oxidation of precursor volatile organic compounds on mineral aerosol surface with increase in ambient water vapor. These results have implications for SOA estimations on regional scales especially in arid and semi–arid regions where significant amount of fine mineral dust is present.

Keywords: Carbonaceous aerosol, secondary organic aerosol, elemental Carbon

Corresponding Author:
Athiyarath K. Sudheer
☎ : +91-79-26314316
🖷 : +91-79-26301502
✉ : sudheer@prl.res.in

1. Introduction

Carbonaceous aerosol, a major contributor to atmospheric fine particulate matter, has potential impact on air quality and regional climate (Menon et al., 2008). Organic aerosol is a poorly understood category that constitutes a substantial portion of ambient aerosol and is ubiquitously present in Earth's atmosphere (Kanakidou et al., 2005). A large fraction of organic aerosol, both natural and anthropogenic, is of secondary origin, produced by oxidation of volatile organic compounds (VOC) (Seinfeld and Pankow, 2003; Zhang et al., 2007; Kroll and Seinfeld, 2008). Secondary organic aerosol (SOA) estimates based on VOC fluxes suggest their dominance over the primary component on a global scale. Though several precursors originate from industrial and automobile emission sources, the dominant fraction of the global SOA budget is thought to be from biogenic VOCs (Kanakidou et al., 2005). Contribution of SOA from anthropogenic precursors to the global SOA budget could be significantly higher than the earlier estimates (de Gouw et al., 2005; Volkamer et al., 2006). However, it has been reported that atmospheric models underestimate organic aerosol mass not only within the boundary layer but at higher altitudes as well (Morris et al., 2006; Goldstein and Galbally, 2007; Yu et al., 2008). The discrepancies associated with these estimated fluxes, as much as an order of magnitude; arise largely due to poor understanding of the formation mechanisms of SOA from the precursors and their controlling factors (Hallquist et al., 2009).

Atmospheric water vapor may impact the concentration of SOA mass, considering equilibrium absorptive partitioning of semi–volatile organic compounds (Seinfeld and Pankow, 2003). Also,

ambient relative humidity is proposed as a factor influencing SOA formation by controlling liquid water content (LWC) in aerosol, which in turn, may promote partitioning of semi–volatile oxidation products of SOA precursors between particle and gas phases and/or heterogeneous reactions of water–soluble organic compounds (Volkamer et al., 2009). Partitioning of carboxylic acids is reported to have a strong influence on RH and it enhances with increase in RH (Falkovich et al., 2004; Hatch et al., 2007). Studies involving simultaneous measurement of particle and gas phase water–soluble organic carbon (WSOC) by Hennigan et al. (2008) revealed that a significant increase in partitioning of WSOC to the particle phase at elevated RH (>70%) occurs. This suggests that such gas–aerosol partitioning of soluble organic compounds and subsequent particle/aqueous phase reactions are important pathway for SOA formation (Ervens et al., 2011). Nguyen et al. (2011) studied effect of RH on isoprene photo–oxidation to produce SOA under humid (90% RH) and dry (<2% RH) conditions. Their results indicated significant change in SOA composition but not any detectable difference in rate and extent of SOA mass increase. In certain circumstances, condensation reactions were suppressed in humid conditions because water is formed as a product as reported by Zhang et al. (2011). Tillmann et al. (2010) studied influence of RH on SOA formation from ozonolysis of α–pinene. Their results provided evidence for increase in SOA yield at humid conditions than at dry conditions. Thus, several reported studies demonstrate, both laboratory experiments as well as field measurements, inconsistencies existing in assessment of effect of RH on SOA formation in ambient atmosphere and need for further investigation on these processes (Dommen et al., 2006; Healy et al., 2009; Zhang et al., 2011).

Numerous compounds contribute to SOA formation and are chemically diverse. Direct measurement technique is not available exclusively for SOA, but various indirect methods are effectively used to infer SOA concentrations. A known ratio of organic carbon (OC) to elemental carbon (EC) for primary emissions has been widely used to estimate SOA (Castro et al., 1999; Pio et al., 2011). SOA production from precursor VOCs is generally through oxidation processes which lead to formation of polar functional groups in product compounds. Hence many of the SOA components are likely to be water–soluble, especially those produced from biogenic VOCs, and hence WSOC in aerosol can be considered as a reasonable proxy for SOA concentration (Kondo et al., 2007; Weber et al., 2007). In this study, we investigate the temporal variation of water vapor content and SOA formation in ambient air. It may be noted that identifying the reactions which dominate the RH effect remains difficult, considering the complexities of different reaction pathways and numerous possible oxidation products of SOA precursors. Thus, we currently rely on proxies such as variation in secondary organic carbon (SOC) and WSOC content as indicators of SOA formation.

2. Experimental Method

$PM_{2.5}$ and PM_{10} samples (particles with aerodynamic diameter <2.5 μm and <10 μm, respectively) were collected on Tissuquartz filters (Pall Life Sciences) using two separate mass–flow controlled high–volume air samplers (Tisch Inc., USA) from March 21 to June 23, 2007 once in a week, at Ahmedabad (23°02'N, 72°32'E), an urban location in a semi–arid region of western India. The two samplers were operated from 09:00 hours (local time) to ~19:00 hours for sampling in daytime and rest of the time were operated for collecting night time samples. There were 26 samples (13 each for $PM_{2.5}$ and PM_{10}) collected during daytime and 24 samples (12 each for $PM_{2.5}$ and PM_{10}) during nighttime (one nighttime sample was not collected on June 7, 2007 due to sampler problem). This set of samples represents the summer season. Another 20 samples (10 each for $PM_{2.5}$ and PM_{10}) were collected during daytime over the period of July to October 2007 which represent monsoon season. Nighttime samples were not collected during the monsoon period. Also, regular weekly sampling was not possible during monsoon season because of intermittent rain events.

Mass loading was ascertained gravimetrically by taking filter weights before and after sampling. Filters were equilibrated at a RH of 40±3% before weighing. The samples were stored under freezing temperature until chemical analysis. The concentrations of EC and OC were measured on EC–OC analyzer (Sunset Laboratory) using NIOSH protocol (Birch and Cary, 1996; Rengarajan et al., 2007). A separate aliquot of samples were treated with HCl fumes in order to eliminate carbonate carbon and analyzed on EC–OC analyzer to apply appropriate correction to OC. These samples were collected using high volume samplers without removing VOCs from the air flow. This can introduce a positive sampling artifact by absorbing VOCs on filters, but the sampling is done for extended time period (typically more than 10 hours) and measured OC content is sufficiently large, hence this artifact is likely to be insignificant. Second aliquot of sample was subjected to microwave digestion with HF and HNO_3; the resultant solution was diluted and analyzed for Al on ICP–MS (Thermo X–series II). A third aliquot of sample was subjected to water extraction and subsequently WSOC and water–soluble ionic species were determined. WSOC was measured on TOC analyzer (Shimadzu, TOC5000A) with NDIR detector. Water–soluble ionic species (K^+, Ca^{2+}, Mg^{2+}, NH_4^+, Na^+, SO_4^{2-}, NO_3^-, Cl^-) were measured on Ion–chromatography system (DIONEX 500) equipped with suppressed conductivity detector. IonPac® CS12 and AS14 analytical columns were used for the separation of ions in cation and anion analysis respectively. Details of the measurement procedures are described elsewhere (Rengarajan et al., 2007).

The measured inorganic ionic species are used in an aerosol thermodynamic equilibrium model, ISORROPIA–II (Fountoukis and Nenes, 2007) (http://nenes.eas.gatech.edu/ISORROPIA/), for calculating the LWC in particulate phase. The model was run as "reverse problem" where particle–phase composition, ambient temperature and relative humidity were used as input. This model was used in earlier studies for calculating H^+ ion concentration as a measure of aerosol acidity at this site and output had shown consistency with experimental results (Rengarajan et al., 2011a). The SOC is estimated by EC–tracer method assuming minimum OC/EC ratio as the primary ratio (Castro et al., 1999). Meteorological parameters i.e., RH, temperature, wind speed and wind direction were obtained from htpp://www.wunderground.com for Ahmedabad station where the data were collected at a location within 10 km from sampling site. The average values of RH and temperature for sampling duration were calculated from the hourly data for all sampling days. Water vapor pressure was calculated at ambient temperature using RH and saturated vapor pressure obtained by IAPWS (International Association for the Properties of Water and Steam) formulation.

We used the MOZART–4 model to calculate OH, CO and NO_X. MOZART–4 (Model for Ozone and Related chemical Tracers, version 4) is a global chemical transport model for the troposphere, simulating 85 gas–phase species and 12 bulk aerosol compounds with the help of 39 photolysis and 157 gas–phase reactions. The chemical mechanism includes an updated isoprene oxidation scheme and treatment of volatile organic compounds. The model is able to reproduce the temporal and spatial distributions of NO_X, CO and OH (Peng and Zhao, 2007; Sheel et al., 2010; Srivastava and Sheel, 2013). Five–day air mass back trajectories were calculated using the Hybrid Single–Particle Lagrangian Integrated Trajectory (HYSPLIT4) model from National Oceanic and Atmospheric Administration (NOAA) using Global Data Assimilation System's global data to identify the origin (Draxler and Rolph, 2013) and transport of air masses prior to the sampling location (for 12:30 hours local time).

3. Results

3.1. PM composition during summer season

The average concentrations of aerosol mass and various constituents during summer are presented in Table 1. Average mass concentration of $PM_{2.5}$ is 39.3 μg m^{-3}, which constitutes ~34% of PM_{10} at Ahmedabad during daytime. The corresponding concentration during nighttime is 47 μg m^{-3}; constituting ~31% of PM_{10}. Total carbonaceous aerosol mass concentration during daytime and nighttime, calculated as [EC+OCx1.6] (Rengarajan et al., 2007), were 13.6 μg m^{-3} and 21.5 μg m^{-3} in $PM_{2.5}$, whereas in PM_{10}, the corresponding concentrations were 19.5 μg m^{-3} and 30.3 μg m^{-3}, respectively. These constitute 34.6% and 45% of $PM_{2.5}$ mass during daytime and at night, while for PM_{10}, these are 16.9% and 20%, respectively. OC/EC ratio ranges from 5.7 to 12.6 in fine mode aerosol during daytime whereas range for nighttime ratio is between 2.4 and 15.6. In comparison with studies reported from European region (Vodicka et al., 2013; Mirante et al., 2014), OC/EC ratios over Indian region are higher due to wide spread emission from biomass combustion for domestic purposes (Gustafsson et al., 2009; Ram and Sarin, 2010). Minimum OC/EC ratios for $PM_{2.5}$ samples (3.0 and 2.4) were observed on 25 April and 23 June for nighttime samples. The minimum ratio was obtained for PM_{10} samples on 25 April (3.3). The ratio of 2.4 and 3.3 are used for calculating SOC in $PM_{2.5}$ and PM_{10} respectively, assuming these as primary ratios, $(OC/EC)_{pri}$, following Castro et al. (1999).

$$SOC = OC - ECx(OC/EC)_{pri} \tag{1}$$

Table 1. *Average concentrations with standard deviation (µg m^{-3}) of aerosol constituents during day and night and their night–to–day ratios in PM$_{2.5}$ and PM$_{10}$ during summer season. During monsoon season, only daytime samples were collected*

|	PM$_{2.5}$ (Summer)			PM$_{10}$ (Summer)			PM$_{2.5}$/PM$_{10}$		Monsoon		
	Day [a] (13)	Night (12)	N/D	Day (13)	Night (12)	N/D	Day	Night	PM$_{2.5}$ (10)	PM$_{10}$ (10)	PM$_{2.5}$/PM$_{10}$
Mass	39.3±10.7	47.4±21	1.2	115±44	152±58	1.3	0.34	0.31	39.2±21	91.8±26	0.43
Cl$^-$	0.17±0.27	1.23±2.3	6.8	1.83±1.8	5.65±3.7	3.1	0.10	0.22	0.25±0.45	2.53±3.0	0.99
NO$_3^-$	0.63±0.41	0.73±0.33	1.1	3.44±1.2	3.32±1.0	1.0	0.19	0.22	0.52±0.38	2.88±0.9	0.18
SO$_4^{2-}$	5.46±1.9	5.80±2.0	1.0	7.96±2.3	8.95±2.8	1.1	0.72	0.65	7.77±4.2	9.22±4.4	0.84
Na$^+$	0.64±0.48	0.97±0.52	1.5	1.91±1.3	3.09±1.9	1.6	0.34	0.31	1.06±0.83	2.73±2.1	0.39
NH$_4^+$	1.07±0.64	1.21±1.2	1.1	0.85±0.62	1.20±1.6	1.4	1.33	1.00	1.66±1.1	1.05±0.85	1.61
K$^+$	0.52±0.19	0.92±0.64	1.7	0.73±0.27	1.29±0.82	1.8	0.74	0.71	0.42±0.25	0.58±0.33	0.72
Mg^{2+}	0.10±0.05	0.13±0.09	1.2	0.39±0.15	0.54±0.17	1.4	0.27	0.24	0.13±0.07	0.42±0.19	0.31
Ca^{2+}	0.62±0.22	0.55±0.27	0.8	4.33±1.6	4.37±1.4	1.0	0.15	0.13	0.74±0.55	3.76±2.43	0.20
EC	0.99±0.7	2.98±2.4	2.9	1.30±0.91	3.59±2.7	2.8	0.79	0.83	1.26±1.1	1.70±1.6	0.74
OC	7.88±3.8	11.6±8.5	1.4	11.9±5.9	16.7±11	1.4	0.68	0.69	7.80±4.1	10.4±7.1	0.75
WSOC	3.65±1.6	3.73±2.0	1.0	4.66±2.8	5.00±3.0	1.1	0.80	0.75	3.40±1.8	3.74±1.4	0.91
SOC	5.52±2.3	4.86±4.6	0.9	7.62±3.3	5.43±4.6	0.7	0.74	0.89	4.77±2.5	4.86±2.3	0.98
OC/EC	8.8±2.2	4.8±3.5		10.1±2.6	5.6±3.2				6.2±2.1	7.35±2.4	

[a] *Value in parentheses is the number of samples collected*

SOC calculated by this method have uncertainties due to following reasons: (i) there may be considerable SOA formation during nighttime when minimum OC/EC is observed; (ii) single data point may not be a true representation of primary emission ratio of the season and (iii) emission sources of carbonaceous species may include varying biomass burning with higher OC/EC ratio. Even though the absolute values of SOC may be under–estimated due to SOA formation when minimum OC/EC ratio was observed, daily variability of SOC can be quantitatively represented with this calculation. The nighttime ratios are consistently lower than day-time values (Table 1) and minimum SOA is more likely to be in nighttime samples. Among nighttime OC/EC ratios, almost 75% values lie between 2 and 4, whereas daytime ratios exhibit wide range (5.7–12.6) allowing day–to–day variability assessment of SOC in this study even though significant uncertainties may be associated with the absolute values. WSOC and SOC exhibit a strong linear correlation, as discussed in Section 4.1, suggesting that the SOC calculated in this study is a reasonable estimate to assess variability in SOA formation. A primary OC/EC ratio of 4.7 was used by Rengarajan et al. (2011a) for SOC calculation at this location which was representative of winter. During winter, biomass burning introduces substantial amount of carbonaceous aerosol in ambient air and the primary OC/EC ratio is expected to be higher.
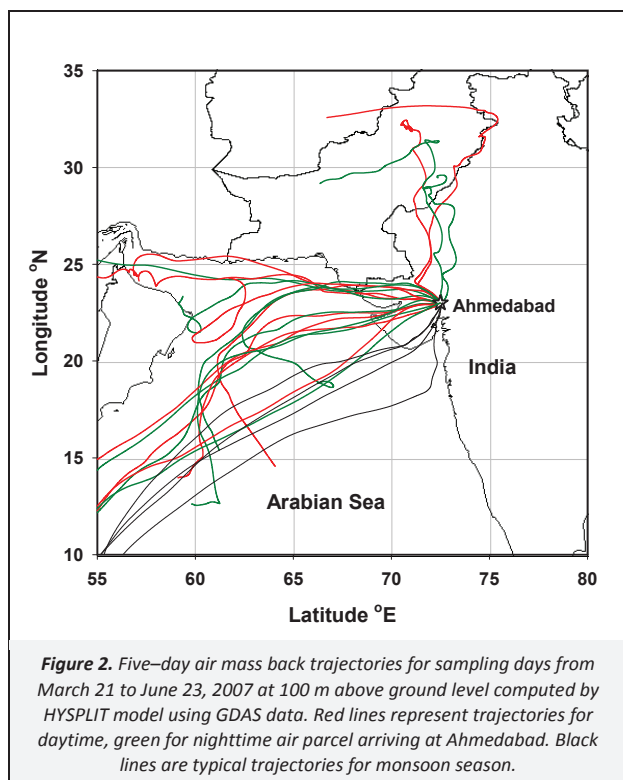
Al is typically considered as a tracer for mineral aerosol (Duce and Tindale, 1991; Kumar et al., 2012). The measured Al concentration in PM$_{2.5}$ averaged at ~0.9 µg m^{-3} with similar concentrations during day and night. Mineral dust concentration estimated (assuming upper continental crust Al abundance, 8%; McLennan, 2001) at the sampling site ranged from 5 to 21 µg m^{-3} (mean: 11±4 µg m^{-3}), which is a significant fraction of PM$_{2.5}$ mass (28%). In PM$_{10}$, mineral dust contributes on an average ~45% of total mass and there is no variation in the percentage contribution in day and night samples. Among inorganic constituents in fine fraction, SO$_4^{2-}$ is the dominant component followed by NH$_4^+$. In PM$_{10}$ also SO$_4^{2-}$ is the most abundant component followed by Ca^{2+}.

During our observation in summer, average daytime RH is less than ~40%, varying from 13 to 36% (except on 6 June 2007; 43%) while nighttime RH was consistently higher, ranging from 29 to 69% (Figure 1). Water vapor pressure was calculated for each sampling day from saturation vapor pressure at observed temperature and RH which varies from 9.2 to 27.1 hPa during daytime. Daytime average temperature ranged from 38.1 to 40.2 °C during sampling (except on 21, March 2007; 31.7 °C). This suggests that the observed variation in average RH is primarily due

to variation in atmospheric water vapor content rather than temperature. LWC calculated for PM$_{2.5}$ samples using thermo-dynamic equilibrium model (ISORROPIA–II) was zero for all the daytime samples except on 6 and 13 June 2007 (~1.3 µg m^{-3}) when the RH values were highest (36 and 43%). During night, LWC varied from 0.3 to 7.9 µg m^{-3} and for two days it was close to zero. LWC was not calculated for PM$_{10}$ samples as coarser particles may not attain equilibrium with gaseous components efficiently compared to fine mode particles. Wind direction during the observation period did not show any distinct pattern during day and night. Generally winds were north westerly or westerly throughout the observation period. Figure 2 depicts the five–day back trajectories of air masses during sampling at 100 m height, indicating that origin and transport of the air mass sampled was, to some extent, over continental areas and substantial time was spent over marine regions. OH concentrations calculated for the sampling time using MOZART model range from 4.4x10^6 to 9.4x10^6 cm^{-3}. The temporal variation of OH radical concentration is similar to that of water vapor content.
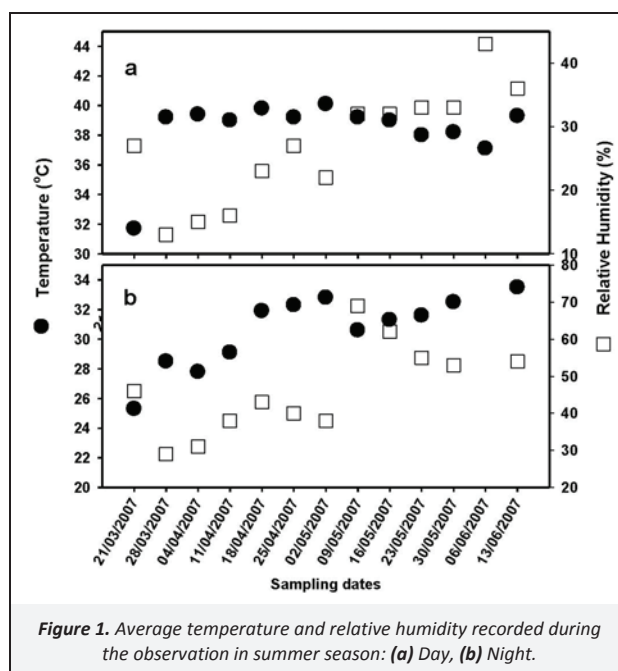
Figure 1. *Average temperature and relative humidity recorded during the observation in summer season: (a) Day, (b) Night.*

Figure 2. Five–day air mass back trajectories for sampling days from March 21 to June 23, 2007 at 100 m above ground level computed by HYSPLIT model using GDAS data. Red lines represent trajectories for daytime, green for nighttime air parcel arriving at Ahmedabad. Black lines are typical trajectories for monsoon season.

3.2. PM composition during monsoon season

Average aerosol mass concentration and various constituents observed during monsoon period are presented in Table 1. The daytime average $PM_{2.5}$ and PM_{10} mass concentrations were 39 µg m^{-3} and 92 µg m^{-3} respectively; comparatively low for PM_{10} with respect to summer season. Total carbonaceous aerosol mass fraction during monsoon period is also similar to that observed in summer, ~37% in $PM_{2.5}$ and ~19% in PM_{10}. SOC was calculated with the same OC/EC minimum ratio observed during summer season. Even though the correlation between SOC and WSOC is not significant in fine fraction, they exhibit a significant linear trend in PM_{10} samples. The average daytime RH were more than 50% except for two days (3 and 18 October, 2007; 41 and 35%, respectively) and maximum value was ~72%. Average temperatures ranging from 31 to 33 °C were recorded. Aerosol LWC is calculated for these days and is significant for all the sampling days except on 3 October, 2007 when the RH was at minimum.

4. Discussion

4.1. Day–night variation in carbonaceous species during summer

Carbonaceous aerosol constitutes a major component of fine particulate mass during summer. Its contributions to total mass during day and night are ~35% and ~45%, respectively. Both EC and OC concentrations are higher during night. Ratio of EC content in $PM_{2.5}$ to that in PM_{10} is ~0.8 and that for OC is ~0.7, demonstrating dominant fraction of carbonaceous aerosol exists as fine mode particles and there is no considerable difference between day and night. Constituents expected to be produced by primary emissions i.e., Na^+, Cl^-, K^+, show higher concentrations at night whereas concentrations of those species from secondary processes (i.e. NH_4^+ and SO_4^{2-}) generally remain constant throughout the day. SOC calculated by EC tracer method shows marginal increase. Increase in aerosol mass as well as concentrations of various constituents at night may be partly due to change in the boundary layer height and lower temperature. It is not possible to delineate this effect quantitatively from emission and formation processes of
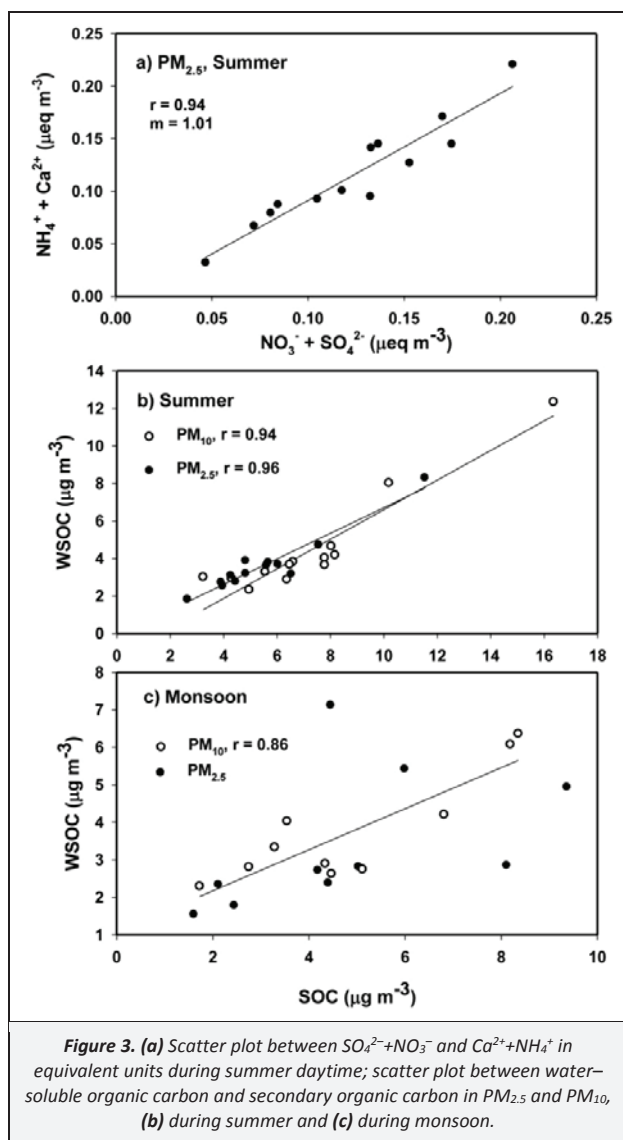
aerosol constituents responsible for their day–night variability; however, comparison of relative proportions of chemical constituents can be used to infer major controlling factors (Ram and Sarin, 2011). Over all, if source strength is constant throughout the diel cycle, nighttime concentrations are expected to be higher than daytime values due to lower boundary layer height. Hence increase in average daytime abundances in any species is due to enhanced formation or emissions compared to nighttime.

The OC/EC ratio in night samples is lower compared to that for day samples. In general, production of SOA is expected to be high during the day by elevated photochemical activities leading to formation of semi–volatile organic compounds that partition to particulate phase. This is corroborated by high daytime WSOC/OC ratios (0.44) when compared to that for night samples (0.32). Rengarajan et al. (2011a) have reported evidence for enhanced SOA formation by presence of acidic aerosol during winter from this location. Aerosol LWC and [H^+] were calculated using ISORROPIA–II model and the results suggest that during summer period the aerosols do not have acidity and mostly are neutral or slightly alkaline in nature. Earlier studies from this location have demonstrated that mineral dust is a major constituent during summer which neutralizes the acidic species like SO_4^{2-} and NO_3^- in this region (Rastogi and Sarin, 2005). Especially during summer period elevated fine dust concentrations are present over this region since it represents a semi–arid region. A scatter plot between ($NO_3^- + SO_4^{2-}$) and ($NH_4^+ + Ca^{2+}$) (Figure 3a), shows a linear relation with a slope of 1.01 and coefficient of regression 0.94. This suggests NH_4^+ and Ca^{2+} present in the aerosol is neutralizing the acidic species almost quantitatively. Also, WSOC exhibits a strong correlation with SOC ($r=0.95$, $p<0.001$ for $PM_{2.5}$ and $r=0.94$, $p<0.001$ for PM_{10}), calculated by EC tracer method, indicating that this can be considered as an independent proxy for SOA (Figure 3b). The ratio of carbonaceous species between $PM_{2.5}$ and PM_{10} samples suggests that the fraction of OC and EC present in coarse mode particles is significant. For example, ~30% of OC and ~20% of EC exist on coarse particles ($PM_{10-2.5}$). Timonen et al. (2008) studied mass size distribution of WSOC from an urban background in Finland and reported enrichment of WSOC in fine and ultra fine particles whereas in coarse mode mass contribution is insignificant. Mineral aerosol abundance in ambient air is comparatively low at the Finland study location and whenever sampling site was influenced by marine air parcel, WSOC is found associated with coarse particles (more than ~2 µm). Estimated dust content from Al concentration at Ahmedabad is ~30% for $PM_{2.5}$ and ~45% for PM_{10} during the sampling period. It is reported earlier that mineral aerosol is the dominant component of atmospheric particulate matter (Rastogi and Sarin, 2005; Rengarajan et al., 2011b). The similar ratio of carbonaceous species between $PM_{2.5}$ and PM_{10} samples collected during day and night indicates that there is no conspicuous change in size distribution during the entire day, over the sampling period (Table 1) compared to that reported by Timonen et al. (2008). Ambient temperature affects the condensation of semi–volatile organic compounds on particulate matter, variation of which can lead to WSOC or SOC concentration changes. Average daytime temperature during the sampling varied in a narrow range (38.2–40.1 °C, except for one day; 31.7 °C) which is not substantial to produce the observed range of variation in SOC. Hence, it can be inferred that during summer, variability in average daytime mass concentrations of SOC and WSOC in ambient aerosol is largely due to changes in SOA formation.

4.2. Effect of relative humidity on SOA formation

Figure 4a shows a linear inverse correlation between SOC and water vapor content ($r=-0.73$, $p<0.01$ for $PM_{2.5}$ and $r=-0.77$, $p<0.005$ for PM_{10}) suggesting that higher atmospheric water vapor content is not favorable for SOA formation in the range of observed RH during daytime in summer; whereas, SOA formation does not exhibit a dependence on ambient water vapor content during nighttime (Figure 4b). There is no significant relation

between SOA and observed water vapor content during monsoon season (Figure 4c). Data points correspond to 35% and 41% RH in monsoon period fall in the same trend of summer period (Figure 4a). Temporal variations in SOC, WSOC and water vapor pressure during the summer sampling period are presented in Figure 5. SOC and WSOC exhibit a general decreasing trend from March to June, whereas water vapor content shows a clear increasing trend. This observation indicates that co–variation of RH and SOC is prominent only during daytime in summer season where the major pathway for SOA formation is through photo-chemical oxidation processes and RH is typically less than 45%.

Figure 3. (a) *Scatter plot between $SO_4^{2-}+NO_3^-$ and $Ca^{2+}+NH_4^+$ in equivalent units during summer daytime; scatter plot between water–soluble organic carbon and secondary organic carbon in $PM_{2.5}$ and PM_{10},* **(b)** *during summer and* **(c)** *during monsoon.*

The decreasing trend of SOA formation with increasing RH or atmospheric water vapor content could be due to the following: (i) local wind direction is favorable to bring air masses with higher atmospheric water vapor as well as lower VOCs, (ii) variation in oxidizing species like OH radicals in ambient air, (iii) in the range of observed RH, SOA formation is inhibited by atmospheric water vapor. During our observation, local wind direction as well as five–day back trajectory analysis (Figure 2) shows that there is no noticeable variation in source region of aerosol and precursor VOCs with respect to RH in summer. Generally, the air masses originated and moved over marine environment (except on 4 and 18 April, 2007) and reached the sampling site through western continental region. Air masses from the western region of the

sampling site are likely to be influenced by marine air with higher RH and have relatively low continentally–derived constituents as well as VOC concentration. In this case, Al concentration during high RH days is expected to be low since marine air will have insignificant amount of Al compared to continental air. Figure 6a presents variation of Al concentrations along with atmospheric water vapor content demonstrating that such a trend is not prevalent. SOA precursor VOCs are known to undergo oxidation processes that are initiated by OH, NO_3 and O_3 or via photolysis, and the oxidation products may have variable impact on O_3–NO_X cycles and radical budget, thus, indirectly affecting SOA formation. Sahu and Lal (2006) reported the seasonal variation of non–methane hydrocarbon abundances at Ahmedabad and argued that this variation was due to changes in transport pattern rather than emission intensities. During summer, as indicated by air mass back trajectories, the transport pattern of air mass remains similar even though RH varied from 15 to 43%. Anthropogenic VOC emissions can have significant influence on SOA formation. Normalizing WSOC with respect to an anthropogenic tracer will avoid bias on comparison due to the possible co–variation of VOC with emission strength. Figure 7a depicts the variation of WSOC concentration normalized to CO mixing ratios which is a typical gas phase anthropogenic tracer simulated by the MOZART model. WSOC/CO also follows the same trend as that of WSOC and SOC during the observation period. This is because the variability in CO is much lower compared to that of WSOC during the observation. Hence, the influence of wind regime and source strength of VOCs is minimal on the observed trend between atmospheric water vapor and SOA.

According to three–dimensional chemical tracer model calculations, OH radical abundance is expected to be maximum during summer and minimum during winter seasons in Northern Hemisphere, particularly in tropical region (Spivakovsky et al., 1990). Simulation with MOZART model had shown that SOA formation can be affected by OH concentration, which in turn is dependent on CO and NO_X abundances (Heald et al., 2008; Su et al., 2012). Figure 7a presents the temporal variation of OH radical concentration during our sampling time, calculated by MOZART model, exhibiting similar trend as that of water vapor content. The average values of O_3 and NO_X mixing ratios are also not showing significant variability during the observation period (Figure 7b). This suggests that, concentrations of oxidizing species in ambient air are increasing during our observation from March to June 2007, and not the limiting factor for VOC oxidation processes for SOA formation. Hence, ambient water vapor content possibly causes a decrease in SOA formation during daytime at lower RH range (<~40%). At higher RH range (>~40%) a direct relation of VOC oxidation and/or SOA formation with ambient water vapor content is not evident (as observed during nighttime as well as during monsoon period).
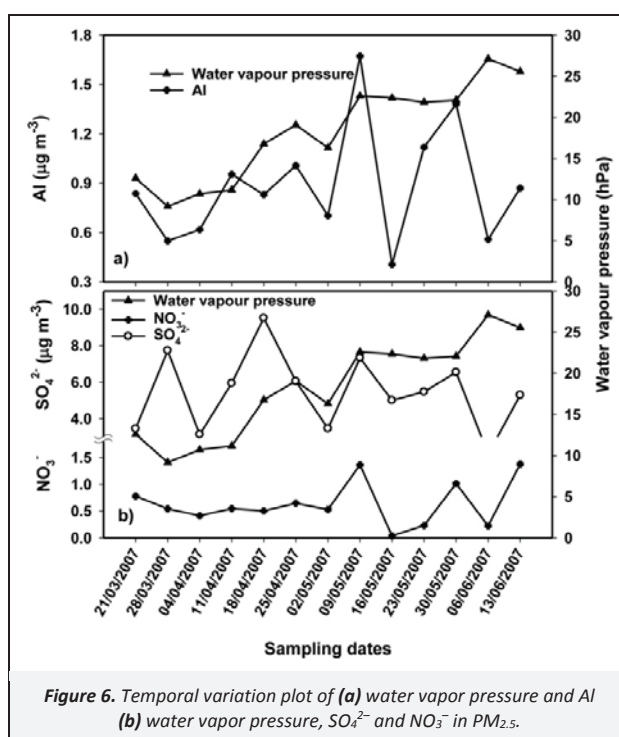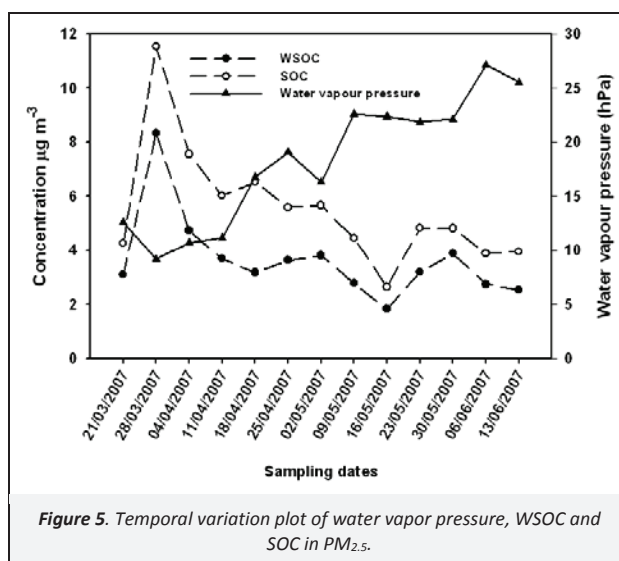
Based on field observations, Hennigan et al. (2008) reported that water uptake by ambient particles may enhance SOA formation by effective partitioning of WSOC onto particles. In these observations, at higher ambient RH (>70%) which allow uptake of water vapor by hygroscopic particles and liquid water content was found favoring the SOA enhancement (Hennigan et al., 2009). Anderson et al. (2008) observed effective partitioning of WSOC during nighttime consistent with increase in RH where average RH was ~90%. Volkamer et al. (2009) demonstrated through laboratory experiments that SOA formation from light non–methane hydrocarbons has a strong dependence on liquid water content of seed aerosol and hence on relative humidity. It is also reported by Healy et al. (2009) that RH, in turn, can control OH radical concentration in presence of NO_X thereby increasing SOA yield from *p*–xylene linearly over RH range of 5–75%. In general, reactive uptake of atmospheric carbonyls produced by oxidation of precursors depends on LWC and hence on RH. However, there is no clear experimental evidence from ambient atmosphere for dependence of SOA formation on RH at lower RH range, where

aerosol LWC is insignificant. In our observation, RH was on the lower range (13–43%) during day time. Thermodynamic equilibrium model, ISORROPIA–II was used to calculate LWC assuming the dominant role of inorganic ionic constituents in water uptake and the results have shown that there is no liquid water during daytime (except on 6 and 13 June 2007) to produce aqueous phase to facilitate SOA formation. At night, RH is relatively higher to produce liquid water content but SOA formation through photochemical processes is not possible and RH effect is not well pronounced. Similarly, during monsoon season, RH has reached up to 72% and most of the sampling days, aerosol LWC was in sufficiently large amount and inverse relation between water vapor content and SOA is not observed. On 3 and 18 October 2007, RH was 41 and 35% respectively and equilibrium model calculation demonstrates that there is no significant amount of LWC. Estimated SOC as well as WSOC during these days also show the same trend with water vapor pressure as obtained during summer sampling (Figure 3a).
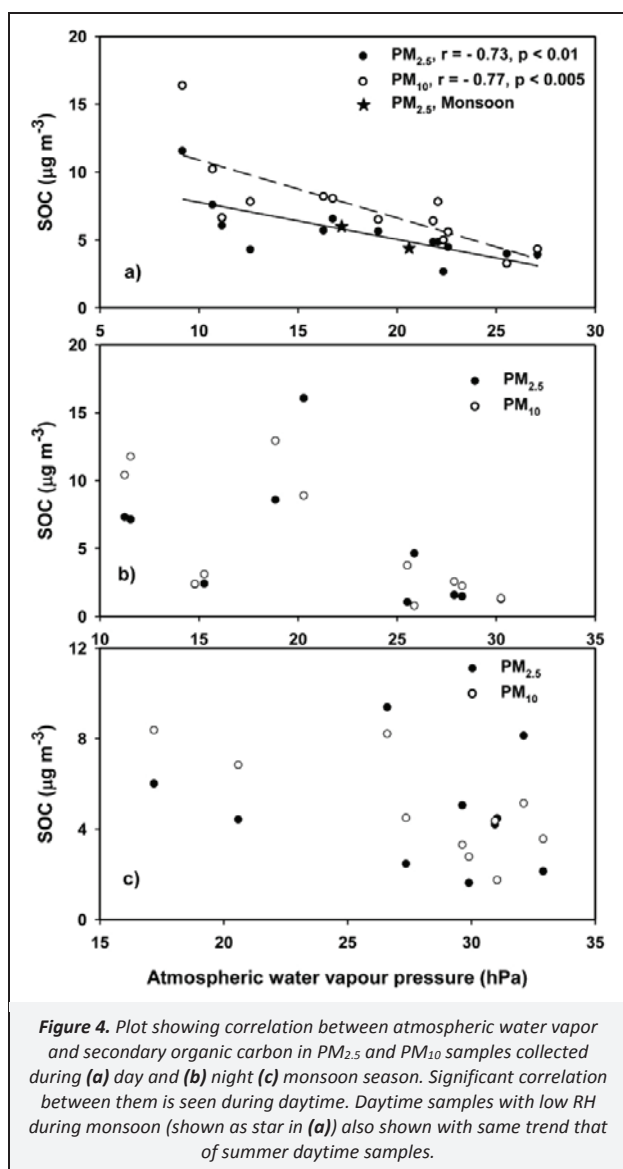
tions. In a recent study, Shakya et al. (2012) observed an inverse correlation between RH and WSOC in New England during summer where the observed average RH was 81%. This was attributed to probable artifact in sampling for 24 hours and a limited number of samples in the regression analysis. In general, aqueous phase oxidation and oligimerization/polymerization reactions lead to increase in SOA mass, as reported from laboratory studies as well as ambient atmosphere. Since water is formed as a product, condensation reactions producing some of the SOA species can get suppressed with increase in LWC content (Nguyen et al., 2011). Zhang et al. (2012) reported SOA is influenced by RH where ambient air is dominated by biogenic VOCs and such dependence is not observed at sampling site where anthropogenic VOC emissions are predominant. The effect is prominent at RH more than ~50% where large amount of LWC is expected. Such a variety of factors may be influencing SOA formation and could be the possible reason for the lack of a positive or negative trend between SOC and RH during nighttime as well as monsoon season.
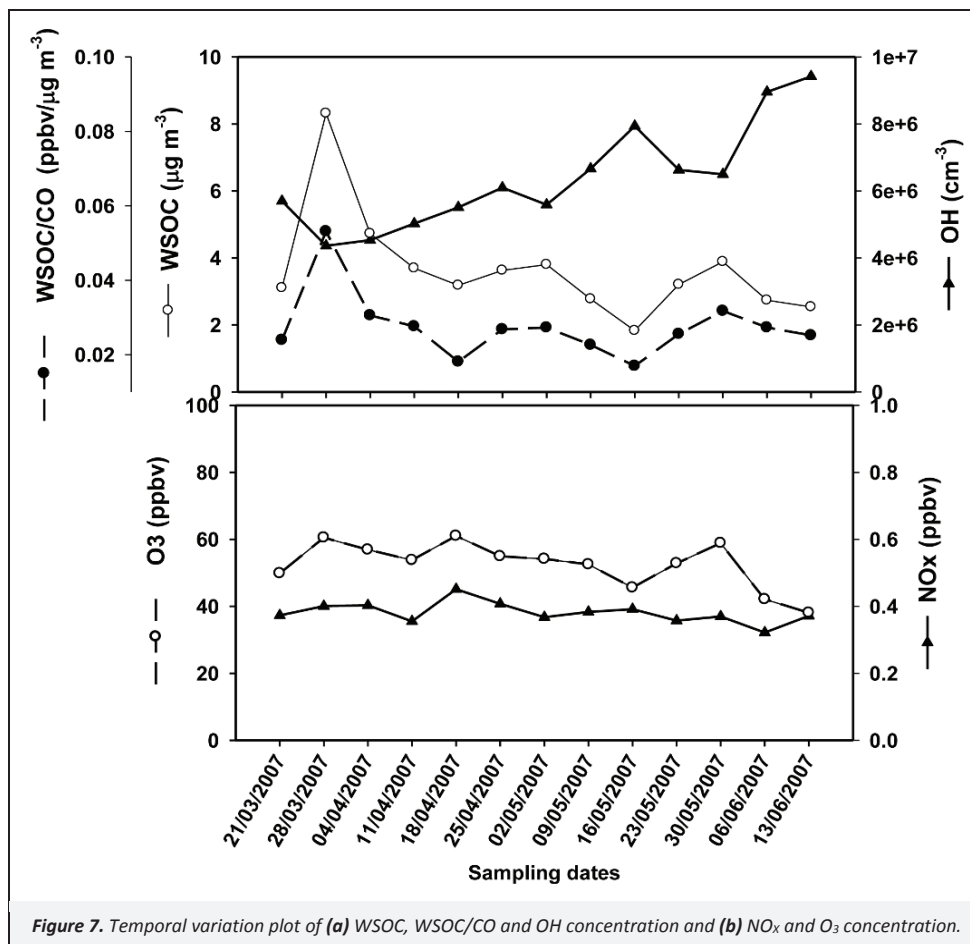

Figure 4. Plot showing correlation between atmospheric water vapor and secondary organic carbon in PM$_{2.5}$ and PM$_{10}$ samples collected during **(a)** day and **(b)** night **(c)** monsoon season. Significant correlation between them is seen during daytime. Daytime samples with low RH during monsoon (shown as star in **(a)**) also shown with same trend that of summer daytime samples.

Figure 5. Temporal variation plot of water vapor pressure, WSOC and SOC in PM$_{2.5}$.

Figure 6. Temporal variation plot of **(a)** water vapor pressure and Al **(b)** water vapor pressure, SO$_4^{2-}$ and NO$_3^-$ in PM$_{2.5}$.

Favez et al. (2008) reported a positive correlation between RH and WSOC/OC ratio at an urban cite in Cairo (Egypt), where ambient RH varied from nearly 30 to 65%. Majority of SOA produced in this region is water–insoluble and attributed to anthropogenic VOC oxidation which is favored at low RH condi-

Figure 7. *Temporal variation plot of **(a)** WSOC, WSOC/CO and OH concentration and **(b)** NO$_x$ and O$_3$ concentration.*

4.3. Role of mineral dust on SOA formation

Inorganic constituents like SO$_4^{2-}$ and NO$_3^-$ do not show any specific trend like SOC and WSOC with atmospheric water vapor content during summer (Figure 6b). Their concentrations show significant variability during our observation (2.07 to 9.52 μg m^{-3} and 0.04 to 1.3 μg m^{-3} respectively) and are expected to be largely formed by secondary process from gaseous precursors. These constituents do not exhibit any significant correlation with WSOC or SOC hence they can be from different sources and/or formation processes. At low RH conditions, homogeneous oxidation is likely to be dominated for the formation of SO$_4^{2-}$ and NO$_3^-$ in ambient particulate matter. But, SOA formation through heterogeneous processes is feasible under a wide range of RH. During summer, mineral dust contributed ~28% of PM$_{2.5}$ mass without significant difference between day and night samples. Ahmedabad, being a typical urban area located in a semi–arid region, has major fraction of mineral dust in ambient aerosol (Rastogi and Sarin, 2005; Rengarajan et al., 2011b). Mineral dust from local emissions may be freshly produced and need not be internally mixed with other constituents, thus providing fresh surface area for adsorption of VOCs to occur. Several laboratory studies on RH dependence of gas/particle partitioning were carried out with aerosol surrogates like soot, combustion products etc. (Jang and Kamens, 1998; Cocker et al., 2001). Mineral surfaces have also been reported to be an efficient sorption phase for organic compounds and the species adsorbed onto the surface are likely to be available for reaction with free radicals or direct photolysis (Gotz et al., 2007). At RH above ~40%, mineral dust is purportedly covered completely by a layer of adsorbed water molecules since minerals present in ambient air are largely hydrophilic or with wettable surfaces (Goss and Eisenreich, 1996) and sorption of VOCs will occur only on/into adsorbed water film. On the other hand, at lower RH range (<~40%) adsorption of VOCs takes place on dry mineral surface sites. Goss and Schwarzenbach (2002) have observed that adsorption of non–polar VOCs on mineral dust surfaces decreases exponentially with increase in RH. For polar compounds, adsorption decreases up to 90% RH and increases afterwards. Many anthropogenic VOCs may be present in substantial amount that can undergo uptake by adsorption on the surface of mineral dust at our study site. Sahu and Lal (2006) demonstrated that seasonal variation of non–methane hydrocarbons at this location is largely due to changes in the transport pattern and boundary layer heights. There is no previous study from this region on natural or biogenic VOCs abundances. Based on ^{14}C measurements of OC, EC, WSOC and water–insoluble organic carbon, SOA formation from biogenic sources are reported to be dominant over anthropogenic sources even in urban regions (Szidat et al., 2009). Vegetation cover in western region of the sampling site especially in Saurashtra region includes deciduous forests that can emit substantial amounts of SOA precursors like isoprene and other reactive biogenic VOCs upwind of Ahmedabad (Panchal and Pandey, 2004; Sharkey et al., 2008; Carlton et al., 2009). Hence the study site is influenced by both anthropogenic and biogenic VOC emissions. The adsorption of these VOCs on dry mineral surfaces leading to SOA formation through heterogeneous processes is a significant pathway during summer. Since the extent of adsorption of VOCs on mineral dust is not favored by increase in RH, significant negative correlation between atmospheric water vapor content and SOC mass concentration is possible as observed in our study. In the case of nighttime samples and monsoon samples, the RH is sufficiently large to produce LWC with soluble inorganic

constituents. In addition to this, mineral dust exists with thin film of water on its surface and inverse relation between atmospheric water vapor content and SOC is not observed. This finding suggests that at low RH range (<~40%) in absence of aerosol LWC, the effect of RH on SOA formation is different if mineral dust is a major component of fine aerosol.

5. Conclusion

The carbonaceous species, water–soluble constituents and mineral dust abundances of $PM_{2.5}$ and PM_{10} were analyzed from an urban location in semi–arid region in western India during summer and monsoon seasons of 2007. SOC calculated by EC–tracer method as well as WSOC exhibit an inverse correlation with atmospheric water vapor content suggesting SOA formation is decreased by presence of atmospheric water vapor during daytime at RH less than ~40%. From this study, we conclude that (i) the mechanism of influence of RH on SOA formation cannot be considered same for the entire ambient RH range, (ii) RH at which liquid water content can exist need to be treated differently, where aqueous phase condensation/oligomerization reactions are possible and (iii) at lower RH values, especially in arid and semi–arid regions where emission and transport of mineral dust are expected, heterogeneous oxidation processes on the mineral dust surfaces may be significant. This in turn may be controlled by relation between RH and adsorption of VOCs on surface of mineral dust depending on their polar nature. The observations reported here has implication in general understanding of organic aerosol, especially SOA formation from precursor VOCs on regional and global scales and emphasizes the need to explore more to identify potential pathways responsible for RH dependence of SOA formation in ambient air for their quantitative representation in models.

Acknowledgments

References

Anderson, C., Dibb, J.E., Griffin, R.J., Bergin, M.H., 2008. Simultaneous measurements of particulate and gas–phase water–soluble organic carbon concentrations at remote and urban–influenced locations. *Geophysical Research Letters* 35, art. no. L13706.

Birch, M.E., Cary, R.A., 1996. Elemental carbon–based method for monitoring occupational exposures to particulate diesel exhaust. *Aerosol Science and Technology* 25, 221–241.

Carlton, A.G., Wiedinmyer, C., Kroll, J.H., 2009. A review of secondary organic aerosol (SOA) formation from isoprene. *Atmospheric Chemistry and Physics* 9, 4987–5005.

Castro, L.M., Pio, C.A., Harrison, R.M., Smith, D.J.T., 1999. Carbonaceous aerosol in urban and rural European atmospheres: Estimation of secondary organic carbon concentrations. *Atmospheric Environment* 33, 2771–2781.

Cocker, D.R., Mader, B.T., Kalberer, M., Flagan, R.C., Seinfeld, J.H., 2001. The effect of water on gas–particle partitioning of secondary organic aerosol: II. *m*–xylene and 1,3,5–trimethylbenzene photooxidation systems. *Atmospheric Environment* 35, 6073–6085.

de Gouw, J.A., Middlebrook, A.M., Warneke, C., Goldan, P.D., Kuster, W.C., Roberts, J.M., Fehsenfeld, F.C., Worsnop, D.R., Canagaratna, M.R., Pszenny, A.A.P., Keene, W.C., Marchewka, M., Bertman, S.B., Bates, T.S., 2005. Budget of organic carbon in a polluted atmosphere: Results from the New England air quality study in 2002. *Journal of Geophysical Research–Atmospheres* 110, art. no. D16305.

Draxler, R.R., Rolph, G.D., 2013. HYSPLIT (HYbrid Single–Particle Lagrangian Integrated Trajectory) Model access via NOAA ARL READY, http://www.arl.noaa.gov/HYSPLIT.php. NOAA Air Resources Laboratory, College Park, MD.

Dommen, J., Metzger, A., Duplissy, J., Kalberer, M., Alfarra, M.R., Gascho, A., Weingartner, E., Prevot, A.S.H., Verheggen, B., Baltensperger, U., 2006. Laboratory observation of oligomers in the aerosol from isoprene/NO_x photooxidation. *Geophysical Research Letters* 33, art. no. L13805.

Duce, R.A., Tindale, N.W., 1991. Atmospheric transport of iron and its deposition in the ocean. *Limnology and Oceanography* 36, 1715–1726.

Ervens, B., Turpin, B.J., Weber, R.J., 2011. Secondary organic aerosol formation in cloud droplets and aqueous particles (AQSOA): A review of laboratory, field and model studies. *Atmospheric Chemistry and Physics* 11, 11069–11102.

Falkovich, A.H., Schkolnik, G., Ganor, E., Rudich, Y., 2004. Adsorption of organic compounds pertinent to urban environments onto mineral dust particles. *Journal of Geophysical Research–Atmospheres* 109, art. no. D02208.

Favez, O., Sciare, J., Cachier, H., Alfaro S. C., Abdelwahab, M. M., 2008. Significant formation of water insoluble secondary organic aerosol in semi–arid urban environment. *Geophysical Research Letters* 35, art. no. L15801.

Fountoukis, C., Nenes, A., 2007. Isorropia II: A computationally efficient thermodynamic equilibrium model for K^+–Ca^{2+}–Mg^{2+}–$NH_4^{(+)}$–Na^+–SO_4^{2-}–NO_3^-–Cl^-–H_2O aerosols. *Atmospheric Chemistry and Physics* 7, 4639–4659.

Goldstein, A. H., Galbally, I. E., 2007. Known and unexplored organic constituents in the Earth's atmosphere. *Environmental Science and Technology* 41, 1514–1521.

Goss, K.U., Schwarzenbach, R.P., 2002. Adsorption of a diverse set of organic vapors on quartz, $CaCO_3$, and alpha–Al_2O_3 at different relative humidities. *Journal of Colloid and Interface Science* 252, 31–41.

Goss, K.U., Eisenreich, S.J., 1996. Adsorption of VOCs from the gas phase to different minerals and a mineral mixture. *Environmental Science & Technology* 30, 2135–2142.

Gotz, C.W., Scheringer, M., Macleod, M., Roth, C.M., Hungerbuhler, K., 2007. Alternative approaches for modeling gas–particle partitioning of semivolatile organic chemicals: Model development and comparison. *Environmental Science & Technology* 41, 1272–1278.

Gustafsson, O., Krusa, M., Zencak, Z., Sheesley, R.J., Granat, L., Engstrom, E., Praveen, P.S., Rao, P.S.P., Leck, C., Rodhe, H., 2009. Brown clouds over south Asia: Biomass or fossil fuel combustion? *Science* 323, 495–498.

Hallquist, M., Wenger, J.C., Baltensperger, U., Rudich, Y., Simpson, D., Claeys, M., Dommen, J., Donahue, N.M., George, C., Goldstein, A.H., Hamilton, J.F., Herrmann, H., Hoffmann, T., Iinuma, Y., Jang, M., Jenkin, M.E., Jimenez, J.L., Kiendler–Scharr, A., Maenhaut, W., McFiggans, G., Mentel, T.F., Monod, A., Prevot, A.S.H., Seinfeld, J.H., Surratt, J.D., Szmigielski, R., Wildt, J., 2009. The formation, properties and impact of secondary organic aerosol: Current and emerging issues. *Atmospheric Chemistry and Physics* 9, 5155–5236.

Hatch, C.D., Gough, R.V., Tolbert, M.A., 2007. Heterogeneous uptake of the C_1 to C_4 organic acids on a swelling clay mineral. *Atmospheric Chemistry and Physics* 7, 4445–4458.

Heald, C.L., Henze, D.K., Horowitz, L.W., Feddema, J., Lamarque, J.F., Guenther, A., Hess, P.G., Vitt, F., Seinfeld, J.H., Goldstein, A.H., Fung, I., 2008. Predicted change in global secondary organic aerosol concentrations in response to future climate, emissions, and land use change. *Journal of Geophysical Research–Atmospheres* 113, art. no. D05211.

Healy, R.M., Temime, B., Kuprovskyte, K., Wenger, J.C., 2009. Effect of relative humidity on gas/particle partitioning and aerosol mass yield in the photooxidation of *p*–xylene. *Environmental Science & Technology* 43, 1884–1889.

Hennigan, C.J., Bergin, M.H., Dibb, J.E., Weber, R.J., 2008. Enhanced secondary organic aerosol formation due to water uptake by fine particles. *Geophysical Research Letters* 35, art. no. L18801.

Hennigan, C.J., Bergin, M.H., Russell, A.G., Nenes, A., Weber, R.J., 2009. Gas/particle partitioning of water–soluble organic aerosol in Atlanta. *Atmospheric Chemistry and Physics* 9, 3613–3628.

Jang, M., Kamens, R. M., 1998. A thermodynamic approach for modeling partitioning of semi–volatile organic compounds on atmospheric particulate matter: Humidity effects. *Environmental Science and Technology* 32, 1237–1243.

Kanakidou, M., Seinfeld, J.H., Pandis, S.N., Barnes, I., Dentener, F.J., Facchini, M.C., Van Dingenen, R., Ervens, B., Nenes, A., Nielsen, C.J., Swietlicki, E., Putaud, J.P., Balkanski, Y., Fuzzi, S., Horth, J., Moortgat, G.K., Winterhalter, R., Myhre, C.E.L., Tsigaridis, K., Vignati, E., Stephanou, E.G., Wilson, J., 2005. Organic aerosol and global climate modelling: A review. *Atmospheric Chemistry and Physics* 5, 1053–1123.

Kondo, Y., Miyazaki, Y., Takegawa, N., Miyakawa, T., Weber, R.J., Jimenez, J.L., Zhang, Q., Worsnop, D.R., 2007. Oxygenated and water–soluble organic aerosols in Tokyo. *Journal of Geophysical Research–Atmospheres* 112, art. no. D01203.

Kroll, J.H., Seinfeld, J.H., 2008. Chemistry of secondary organic aerosol: Formation and evolution of low–volatility organics in the atmosphere. *Atmospheric Environment* 42, 3593–3624.

Kumar, A., Sudheer, A.K., Goswami, V., Bhushan, R., 2012. Influence of continental outflow on aerosol chemical characteristics over the Arabian sea during winter. *Atmospheric Environment* 50, 182–191.

McLennan, S.M., 2001. Relationships between the trace element composition of sedimentary rocks and upper continental crust. *Geochemistry Geophysics Geosystems* 2, art. no. 2000GC000109.

Menon, S., Unger, N., Koch, D., Francis, J., Garrett, T., Sednev, I., Shindell, D., Streets, D., 2008. Aerosol climate effects and air quality impacts from 1980 to 2030. *Environmental Research Letters* 3, art. no. 024004.

Mirante, F., Salvador, P., Pio, C., Alves, C., Artinano, B., Caseiro, A., Revuelta, M.A., 2014. Size fractionated aerosol composition at roadside and background environments in the Madrid urban atmosphere. *Atmospheric Research* 138, 278–292.

Morris, R.E., Koo, B., Guenther, A., Yarwood, G., McNally, D., Tesche, T.W., Tonnesen, G., Boylan, J., Brewer, P., 2006. Model sensitivity evaluation for organic carbon using two multi–pollutant air quality models that simulate regional haze in the Southeastern United States. *Atmospheric Environment* 40, 4960–4972.

Nguyen, T.B., Roach, P.J., Laskin, J., Laskin, A., Nizkorodov, S.A., 2011. Effect of humidity on the composition of isoprene photooxidation secondary organic aerosol. *Atmospheric Chemistry and Physics* 11, 6931–6944.

Panchal, N. S., Pandey, A. N., 2004. Analysis of vegetation of Rampara forest in Saurashtra region of Gujarat state of India. *Tropical Ecology* 45, 223–231.

Peng, L., Zhao, C.S., 2007. Analysis of carbon monoxide budget in North China. *Chemosphere* 66, 1383–1389.

Pio, C., Cerqueira, M., Harrison, R.M., Nunes, T., Mirante, F., Alves, C., Oliveira, C., de la Campa, A.S., Artinano, B., Matos, M., 2011. OC/EC ratio observations in Europe: Re–thinking the approach for apportionment between primary and secondary organic carbon. *Atmospheric Environment* 45, 6121–6132.

Ram, K., Sarin, M.M., 2011. Day–night variability of EC, OC, WSOC and inorganic ions in urban environment of Indo–Gangetic plain: Implications to secondary aerosol formation. *Atmospheric Environment* 45, 460–468.

Ram, K., Sarin, M.M., 2010. Spatio–temporal variability in atmospheric abundances of EC, OC and WSOC over Northern India. *Journal of Aerosol Science* 41, 88–98.

Rastogi, N., Sarin, M.M., 2005. Long–term characterization of ionic species in aerosols from urban and high–altitude sites in Western India: Role of mineral dust and anthropogenic sources. *Atmospheric Environment* 39, 5541–5554.

Rengarajan, R., Sudheer, A.K., Sarin, M.M., 2011a. Aerosol acidity and secondary organic aerosol formation during wintertime over urban environment in Western India. *Atmospheric Environment* 45, 1940–1945.

Rengarajan, R., Sudheer, A.K., Sarin, M.M., 2011b. Wintertime $PM_{2.5}$ and PM_{10} carbonaceous and inorganic constituents from urban site in western India. *Atmospheric Research* 102, 420–431.

Rengarajan, R., Sarin, M.M., Sudheer, A.K., 2007. Carbonaceous and inorganic species in atmospheric aerosols during wintertime over urban and high–altitude sites in North India. *Journal of Geophysical Research–Atmospheres* 112, art. no. D21307.

Sahu, L. K., Lal, S., 2006. Distribution of C_2–C_5 NMHCs and related trace gases at a tropical urban site in India. *Atmospheric Environment* 40, 880–891.

Seinfeld, J.H., Pankow, J.F., 2003. Organic atmospheric particulate material. *Annual Review of Physical Chemistry* 54, 121–140.

Shakya, K.M., Place, P.F., Griffin, R.J., Talbot, R.W., 2012. Carbonaceous content and water–soluble organic functionality of atmospheric aerosols at a semi–rural New England location. *Journal of Geophysical Research–Atmospheres* 117, art. no. D03301.

Sharkey, T.D., Wiberley, A.E., Donohue, A.R., 2008. Isoprene emission from plants: Why and how. *Annals of Botany* 101, 5–18.

Sheel, V., Lal, S., Richter, A., Burrows, J.P., 2010. Comparison of satellite observed tropospheric NO_2 over India with model simulations. *Atmospheric Environment* 44, 3314–3321.

Spivakovsky, C.M., Yevich, R., Logan, J.A., Wofsy, S.C., Mcelroy, M.B., Prather, M.J., 1990. Tropospheric OH in a 3–dimensional chemical tracer model – an assessment based on observations of CH_3CCl_3. *Journal of Geophysical Research–Atmospheres* 95, 18441–18471.

Srivastava, S., Sheel, V., 2013. Study of tropospheric CO and O_3 enhancement episode over Indonesia during autumn 2006 using the model for ozone and related chemical tracers (MOZART–4). *Atmospheric Environment* 67, 53–62.

Su, M.F., Lin, Y.P., Fan, X.Q., Peng, L., Zhao, C.S., 2012. Impacts of global emissions of CO, NO_x, and CH_4 on China tropospheric hydroxyl free radicals. *Advances in Atmospheric Sciences* 29, 838–854.

Szidat, S., Ruff, M., Perron, N., Wacker, L., Synal, H.A., Hallquist, M., Shannigrahi, A.S., Yttri, K.E., Dye, C., Simpson, D., 2009. Fossil and non–fossil sources of organic carbon (OC) and elemental carbon (EC) in Goteborg, Sweden. *Atmospheric Chemistry and Physics* 9, 1521–1535.

Tillmann, R., Hallquist, M., Jonsson, A.M., Kiendler–Scharr, A., Saathoff, H., Iinuma, Y., Mentel, T.F., 2010. Influence of relative humidity and temperature on the production of pinonaldehyde and OH radicals from the ozonolysis of alpha–pinene. *Atmospheric Chemistry and Physics* 10, 7057–7072.

Timonen, H., Saarikoski, S., Tolonen–Kivimaki, O., Aurela, M., Saarnio, K., Petaja, T., Aalto, P.P., Kulmala, M., Pakkanen, T., Hillamo, R., 2008. Size distributions, sources and source areas of water–soluble organic carbon in urban background air. *Atmospheric Chemistry and Physics* 8, 5635–5647.

Vodicka, P., Schwarz, J., Zdimal, V., 2013. Analysis of one year's OC/EC data at a Prague suburban site with 2–h time resolution. *Atmospheric Environment* 77, 865–872.

Volkamer, R., Ziemann, P.J., Molina, M.J., 2009. Secondary organic aerosol formation from acetylene (C_2H_2): Seed effect on SOA yields due to organic photochemistry in the aerosol aqueous phase. *Atmospheric Chemistry and Physics* 9, 1907–1928.

Volkamer, R., Jimenez, J.L., San Martini, F., Dzepina, K., Zhang, Q., Salcedo, D., Molina, L.T., Worsnop, D.R., Molina, M.J., 2006. Secondary organic aerosol formation from anthropogenic air pollution: Rapid and higher than expected. *Geophysical Research Letters* 33, art. no. L17811.

Weber, R.J., Sullivan, A.P., Peltier, R.E., Russell, A., Yan, B., Zheng, M., de Gouw, J., Warneke, C., Brock, C., Holloway, J.S., Atlas, E.L., Edgerton, E., 2007. A study of secondary organic aerosol formation in the anthropogenic–influenced Southeastern United States. *Journal of Geophysical Research–Atmospheres* 112, art. no. D13302.

Yu, S. C., Mathur, R., Schere, K., Kang, D. W., Pleim, J., Young, J., Tong, D., Pouliot, G., McKeen, S. A., Rao, S. T., 2008. Evaluation of real–time PM$_{2.5}$ forecasts and process analysis for PM$_{2.5}$ formation over the eastern United States using the Eta–CMAQ forecast model during the 2004 ICARTT study. *Journal of Geophysical Research–Atmosphere* 113, art. no. D06204.

Zhang, X.L., Liu, J.M., Parker, E.T., Hayes, P.L., Jimenez, J.L., de Gouw, J.A., Flynn, J.H., Grossberg, N., Lefer, B.L., Weber, R.J., 2012. On the gas–particle partitioning of soluble organic aerosol in two urban atmospheres with contrasting emissions: 1. Bulk water–soluble organic carbon. *Journal of Geophysical Research–Atmospheres* 117, art. no. D00V16.

Zhang, H., Surratt, J.D., Lin, Y.H., Bapat, J., Kamens, R.M., 2011. Effect of relative humidity on SOA formation from isoprene/NO photooxidation: Enhancement of 2–methylglyceric acid and its corresponding oligoesters under dry conditions. *Atmospheric Chemistry and Physics* 11, 6411–6424.

Zhang, Q., J. L. Jimenez, M. R. Canagaratna, J. D. Allan, H. Coe, I. Ulbrich, M. R. Alfarra, A. Takami, A. M. Middlebrook, Y. L. Sun, K. Dzepina, E. Dunlea, K. Docherty, P. F. DeCarlo, D. Salcedo, T. Onasch, J. T. Jayne, T. Miyoshi, A. Shimono, S. Hatakeyama, N. Takegawa, Y. Kondo, J. Schneider, F. Drewnick, S. Borrmann, S. Weimer, K. Demerjian, P. Williams, K. Bower, R. Bahreini, L. Cottrell, R. J. Griffin, J. Rautiainen, J. Y. Sun, Y. M. Zhang, D. R. Worsnop, 2007. Ubiquity and dominance of oxygenated species in organic aerosol in anthropogenically–influenced Northern Hemisphere midlatitudes. *Geophysical Research Letters* 34, art. no. L13801.